

NUMERICAL SIMULATION OF COUPLING COEFFICIENT OF APERTURES IN MISSILE ENCLOSURE

¹CHAO MAO, ¹JIJIN TONG, ¹ZHONG LIU, ²ZHIMING QIU

¹School of Electronic Engineering, Naval University of Engineering, Wuhan 43033, Hubei, China

²System Division, Navy Academy of Armament, Beijing 10073, Beijing, China

ABSTRACT

Aperture coupling is the main coupling mode through which electromagnetic pulse (EMP), ultra wideband (UWB) and high power microwave (HPM) can disturb or damage electronic equipments of the missile enclosure. To get knowledge of the coupling effects of apertures with different shapes and positions, coupling processes of HPM into the missile enclosure are investigated. The simulation results indicate that: the axial direction coupling coefficient is larger than the radial direction coupling coefficient. So to damage the electronic system of the missile better, the incident wave should be axial direction.

Keywords: *Missile Enclosure, Aperture Coupling, Finite Element Method, Coupling Coefficient*

1. INTRODUCTION

The electromagnetic pulse (EMP), ultra wideband (UWB) and high power microwave (HPM) can disturb or damage electronic system and equipments with coupling effects. The susceptibility investigations of different electronic systems are the important issue in EMC and EMI. In order to classify the different failure effects, from interference only during the RF illumination to permanent damages, the two quantities breakdown failure rate (BFR) and destruction failure rate (DFR) were defined. In fact, these quantities describe failure effects of single components and subsystems very well, but it seems to be reasonable to extent the classification to the total system and to assess the mission impact. In case of a time critical system like a missile, a small basic cause without any physical damage of an electronic component (e.g. self reset of a microcontroller) could lead to the destruction of the complete system due to a crash.

The electronic systems in the missile are so intensively, precisely and intelligent that the anti-susceptibility is decreased. The feasibility of the electromagnetic damage for the missile increase dramatically. The coupling electromagnetic energy through the apertures, which could not be avoided at the missile body, causes the key electronic equipments failures or damages [1]. In order to predict the immunity of a missile against different electromagnetic threats, not only the electronic system but also the enclosure has to be taken into consideration. Therefore in search of the effective

radiation to damage the missile, the law of the electromagnetic pulse coupling effects should be investigated.

In [2] the analytical description and experimental verification of a cavity with small apertures were given. In [3-5] the aperture coupling effects at the front side have investigated. But the investigation of the aperture array coupling and the coupling effects at the cylindrical surface is not so much as the coupling effects at the front side.

A number of computational methods have been proposed for the solution of shielding problems, including the finite-difference time-domain (FDTD) method, the method of moments (MOM), and the finite element method (FEM) [6]. In this paper, the coupling effect of a missile enclosure is investigated by finite element method (FEM). To compare the coupling effectiveness, a metallic hollow cylinder is equipped with different dimension, different shape, different location apertures and aperture array.

2. THEORETICAL BACKGROUND

A metallic tube respectively a hollow cylinder was used a simple model of the missile cabin enclosure. Since the length L of the enclosure is many times larger than its diameter D , the enclosure can be treated as a cylindrical waveguide.

2.1 Cylindrical Waveguides

The characteristic electrical quantity of waveguides is the cut-off frequency f_c of a certain mode. In case of a cylindrical waveguide it is given for transverse electrical modes by

$$f_{mnl} = \frac{c}{2\pi\sqrt{\mu_r\epsilon_r}} \sqrt{\left(\frac{p_{mn}}{a}\right)^2 + \left(\frac{l\pi}{L}\right)^2} \quad (1)$$

Where f_{mnl} is the resonance frequency of the TE_{mnl} mode.

$$f'_{mnl} = \frac{c}{2\pi\sqrt{\mu_r\epsilon_r}} \sqrt{\left(\frac{p'_{mn}}{a}\right)^2 + \left(\frac{l\pi}{L}\right)^2} \quad (2)$$

Where f'_{mnl} is the resonance frequency of the TM_{mnl} mode.

In (1) and (2), m, n are integers, L is the length of the metallic tube and $a = D/2$ is the radius of the metallic tube. p_{mn} and p'_{mn} are the n^{th} roots of the Bessel function $J_m(x)$ and its deviation $J'_m(x)$. ϵ_r and μ_r are the relative permittivity respectively permeability of the material inside the waveguide and c is the speed of the light. Table I gives an overview about the first TE_{mn} - and TM_{mn} -modes that are able to propagate inside the metallic tube and their resonance frequencies.

2.2 Definition of Coupling Coefficient

η (Coupling coefficient) is used to value the effect of shielding in electromagnetic coupling problems of cavities with apertures. The definition of η is based on a plane wave excitation and the following procedure.

Excite the cavity with an incident pulse plane wave and record the electric field at the certain position.

Excite an empty space computational domain with the same incident pulse plane wave and record the electric field at the same position.

Fourier transforms the time domain data.

$$\eta = 20\lg(E_s/E_0) \quad (3)$$

Where E_0 is the empty space electric field, E_s is the problem space electric field.

2.3 Finite Elements Methods

The EM simulation is based on FEM, understanding the theory will be helpful for the problem. A fictitious surface is introduced surrounding the enclosure when analysing electromagnetic field with finite element method.

Sommerfeld radiation condition

$$\hat{n} \times (\nabla \times \bar{E}^{sc}) + jk_0 \hat{n} \times (\hat{n} \times \bar{E}^{sc}) = 0 \quad (4)$$

Where $\bar{P}(\bar{E}^{sc}) = jk_0 \hat{n} \times (\hat{n} \times \bar{E}^{sc})$.

$$\hat{n} \times (\nabla \times \bar{E}^{sc}) + \bar{P}(\hat{n} \times \bar{E}^{sc}) = 0 \quad (5)$$

Calculating the electric field of the enclosure with apertures, it should meet the vector wave equation in the interior of the enclosure.

$$\nabla \times \left(\frac{1}{\mu_r} \nabla \times \bar{E} \right) - k_0^2 \epsilon_r \bar{E} = 0 \quad (6)$$

In the cavity wall, tangential electric field set zero. Then

$$\hat{n} \times \bar{E} = 0 \quad (7)$$

Openings in the enclosure, the tangential electric and magnetic fields in the cavity openings should be continuous.

$$\hat{z} \times \bar{E} \Big|_{z=0^+} = \hat{z} \times \bar{E} \Big|_{z=0^-} \quad (8)$$

$$z \times [\nabla \times \bar{E}] \Big|_{z=0^+} = z \times \left[\frac{1}{\mu_r} \nabla \times \bar{E} \right] \Big|_{z=0^-} \quad (9)$$

We can obtain the electric field value by choosing appropriate interpolation unction using the boundary conditions for solving equations.

3. SIMULATIONS

3.1 Physical Model

The parameters of the missile enclosure are the length $L=80\text{cm}$, the diameter $D=34.4\text{cm}$, the wall thickness $r=2\text{mm}$. As shown in Fig. 1, the metallic tube could be equipped with different shape apertures at one end and terminations on the other and with different shape apertures at the cylindrical surface with the two termination. The termination of the other end of the tube was short. The complete metallic structure was ideal conducting. The absorbing boundary is two times larger than the missile cabin enclosure. and was illuminated by an incident electromagnetic wave as shown in Fig. 1.

(1) In order to calculate the coupling coefficient due to the different position as the front side and the cylindrical surface, the metallic structure was illuminated by an incident electromagnetic wave from the axial direction and the radial direction respectively. The rectangular coordinate system for the model was set up as shown in Fig.1. The direction of the incident plane waves are the positive directions of X-axis and Y-axis respectively. Slot I at the front side and slot II at the cylindrical surface are shown in Fig. 1.

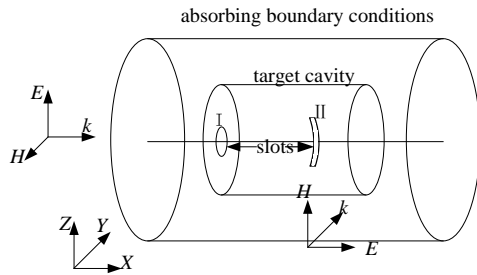


Figure 1: Principle Build Up Of The Missile Cavity Model

(2) In order to calculate the coupling coefficient due to the printed-circuit board in the missile enclosure, the metallic structure was illuminated by an incident electromagnetic wave from the axial direction. The rectangular coordinate system for the model was set up as shown in Fig.1. The direction of the incident plane waves are the positive directions of X-axis and Y-axis respectively. Slot I at the front side is circular aperture. The PCB centre is located at the axial cord. The distance between the PCB and the slot is L . The length of the parallel micro strip is h .

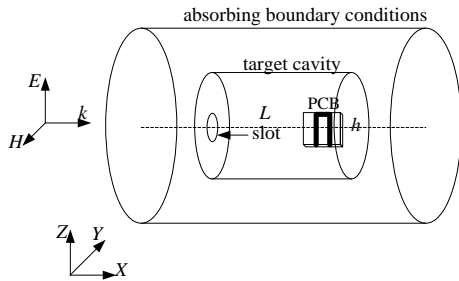


Figure 2: Principle Build Up Of The PCB In The Missile Cavity Model

3.2 Different Shape Apertures at the Front Side

This section analyses the coupling coefficient η of the missile cabin enclosure with the different shape apertures at the front side. Six cases are at same position, as shown in Fig. 3. There are square aperture, rectangular aperture, elliptical aperture, circular aperture, triangular aperture and square array apertures. The parameters of the apertures are shown in Fig. 3. The area of the different shape apertures is 100mm^2 all the same. For the rectangular aperture, the electric field direction was against to the long side as shown in Fig. 1.

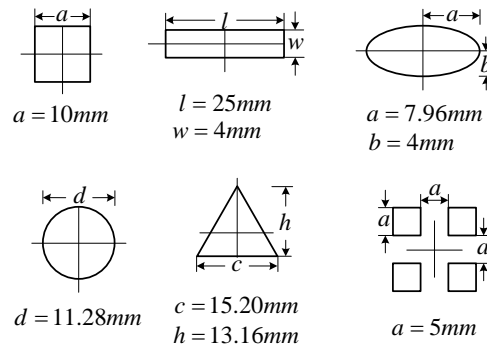


Figure 3: Different Shape Slots At Front Side

3.3 Different Shape Apertures at the Cylindrical Surface

This section analyses the coupling coefficient η of the missile cabin enclosure with the different shape apertures at the cylindrical surface. Three cases are at same position, as shown in Fig. 4. There are square aperture, rectangular aperture and square array apertures. The parameters of the apertures are shown in Fig. 4. The area of the different shape apertures is 100mm^2 all the same. For the rectangular aperture, the electric field direction was against to the long side as shown in Fig. 1.

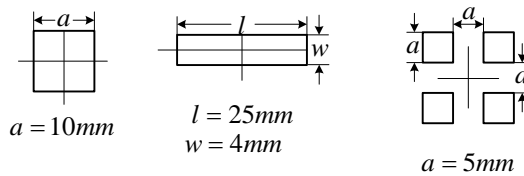


Figure 4: Different Shape Slots At Cylindrical Surface

3.4 Different Micro-strip Line Topologies at the Axial Cord

This section analyses the coupling coefficient η of the missile cabin enclosure with the different micro-strip line topologies at the axial cord. The area of the circular aperture is 100mm^2 at the front side. Five cases are simulated as shown in Fig.5. The parameters of the micro-strip line are the length and the distance from the slot. The different topologies are shown in Fig. 5.

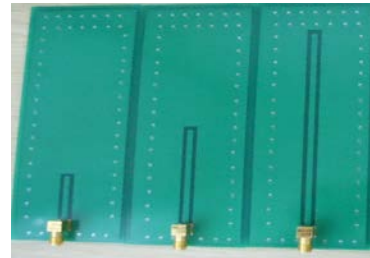


Figure 5: Different Micro-Strip Line Topologies

3.5 Simulation Results

To validate the accuracy of FEM program used in this paper, consider the shielding effectiveness of a 30×12×30cm rectangular metallic cavity with a circular aperture. The simulation result is shown as Fig. 6. The resonance frequency of the cavity is 0.7GHz, coincide with the results in [7]. It indicates the FEM program used in this paper is accurate.

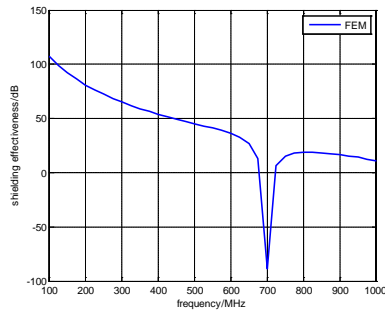


Figure 6: The Comparison Of Rectangular Cavity's Shielding Effectiveness

This section analyses the coupling coefficient η of the missile cabin enclosure with the different shape apertures at the front side. The origin of the used coordinate system is located in the middle of the front side, while the x-axis forms the symmetry axis of the metallic cylinder. The cylinder was excited by a TEM-wave as shown in Fig. 1. The amplitude of the electric field was $E = 1 \text{ kV/m}$.

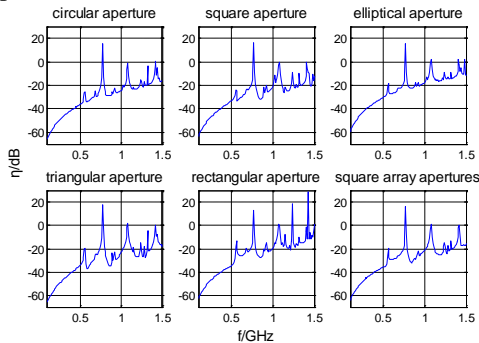


Figure 7: Coupling Coefficient Of Different Shape Slots At Front Side

Six cases are at same position, as shown in Fig.7. Fig.7 shows a rapid increase of the coupling coefficient η at the resonance frequency of the fundamental mode at approximately 0.549GHz for the observation point. A detailed analysis of the component in propagation direction leads to another interesting result. While a first increase of the gain is at 0.55GHz, a second rapid increase occurs at approximately 0.69GHz. According to table I, the resonance frequency of the TM_{01} -Mode is $f'_{011}=0.699\text{GHz}$. This mode is the second mode

that is able to propagate and the first one that has an electric field component in propagation direction.

As the six cases shows in Fig.7, the coupling coefficient η of the triangular and rectangular aperture is higher than the other ones. The high frequency of the incident plane wave is easier to coupling into the missile enclosure with the millimetre-sized apertures.

This section analyses the coupling coefficient η of the missile cabin enclosure with the different shape apertures at the cylindrical surface. Three cases are at same position, as shown in Fig.8. Fig.8 shows a rapid increase of the coupling coefficient η at the resonance frequency of the fundamental mode at approximately 0.55GHz for the observation point as the front side case. Compare to the simulation results of apertures at the front side, the resonance frequency of the TM_{01} -Mode is $f'_{011} = 0.699\text{GHz}$ dramatically ever more with the aperture at the cylindrical surface.

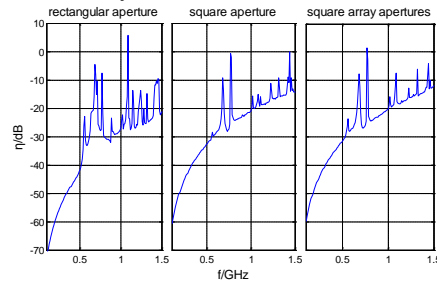


Figure 8: Coupling Coefficient Of Different Shape Slots At Cylindrical Surface

This section analyses the coupling coefficient η of the missile cabin enclosure with/without the PCB. Fig.9 shows a rapid increase of the coupling coefficient η for the PCB in the missile cabin enclosure. The resonance frequency of the fundamental mode is approximately 0.5GHz for the observation point. The simulation result indicates that the PCB cause the advancing of the missile cabin resonance point and the improving of the coupling coefficient. Fig. 10 shows the coupling coefficient variation curve as the PCB at the different locations. The coupling coefficient as the location of the PCB changing is not obviously. It is concluded that the function for the location of the PCB is weak correlation of the coupling coefficient.

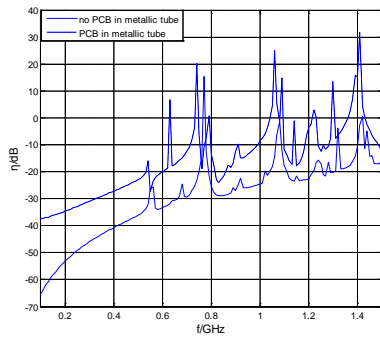


Figure 9: Coupling Coefficient Of Slot With/Without Internal PCB

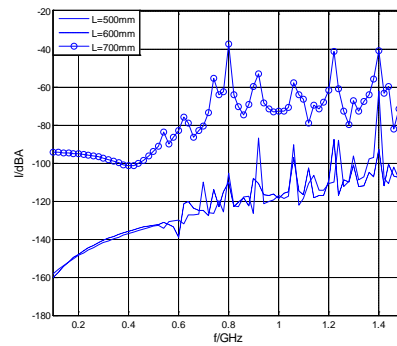


Figure 11: Induced Current As The PCB At Different Locations Interior Cavity

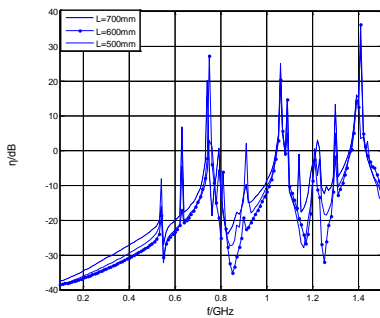


Figure 10: Coupling Coefficient As The PCB At Different Locations

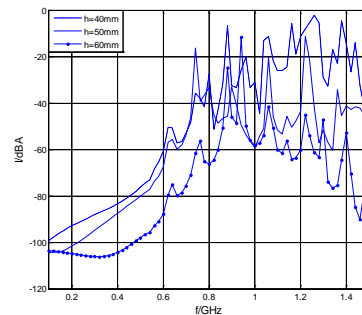


Figure 12: Induced Current As The Changing Of The Micro Strip Line Length

This section analyses the induced current for the changing of the PCB's location in the micro strip current as the coupling electromagnetic energy in the missile enclosure. Fig.11 shows the induced current variation curve as the PCB at the different locations. The induced current with the $L=500\text{mm}$ is little difference from the $L=600\text{mm}$. But when the L is equal to 700mm , the induced current has a great upgrade. From the Fig.10, the changing of the PCB's location has little influence on the coupling coefficient, so the induced current in the micro strip current is sensitively to the PCB's location.

This section analyses the induced current for the changing of the micro strip's length in the micro strip current as the coupling electromagnetic energy in the missile enclosure. Fig.12 shows the induced current variation curve as the different micro strip's length. As the shorten of the micro strip's length, the induced current becomes larger.

4. CONCLUSIONS

In this paper the coupling coefficient properties of a missile enclosure was investigated by means of a metallic hollow cylinder equipped with different shape millimetre-sized apertures at the front side, the cylindrical surface and internal PCB. Among the single aperture, the square and circle aperture is lower than the other shape apertures at the high frequency. The square array apertures' coupling coefficient is lower than the other shape apertures both at the front side and the cylindrical surface. The simulation results indicate that the high power microwave with axial direction incidence is easier to couple into the missile enclosure with the millimetre-sized apertures at the front side than the apertures at the cylindrical surface. Within the internal PCB, the coupling coefficient is higher than the case empty.

To enhance the high power microwave damage, the incident wave should be directed at the missile axial direction as the same shape aperture at the front side and the cylindrical surface.



REFERENCES:

- [1] M. Camp, H. Garbe, D. Nitsch, "UWB and EMP susceptibility of modern electronic", *Proceedings of IEEE International Symposium on Electromagnetic Compatibility*, 2001, Vol. 2, pp. 1015-1020.
- [2] G. Gerri, R. D. Leo, V. Mprimiani, "Theoretical and experimental evaluation of the electromagnetic radiation from apertures in shielded enclosures", *IEEE Trans. on Electromagnetic Compatibility*, Vol. EMC-34, No.4, 1992, pp.423-432.
- [3] M. Edrisi, W. K. Chan, "EMC methodology for numerical electric field computation inside enclosure with aperture", *Electronic Letters*, Vol.35, 1999, pp.1233-1235.
- [4] S. Fisahn, H. Garbe, "Protective properties of a missile enclosure against electromagnetic influences", *Advances in Radio Science*, No. 5, 2007, pp. 63-67.
- [5] C. H. Liang, D. K. Cheng, "Electromagnetic fields coupled into a cavity with a slot-aperture under resonant conditions", *IEEE Trans. on Antennas Propagat.*, Vol. AP-30, 1982, pp.664-672.
- [6] M. Li, J. Nuebel, J. L. Drewniak, et al, "EMI from airflow aperture arrays in shielding enclosure-experiments, FDTD, and MoM modeling", *IEEE Trans on Electromagnetic Compatibility*, Vol. 24, No.3, 2000, pp.265-275.
- [7] M. P. Robinson, M. T. Benson, C. Christopoulos, et al, "Analytical formulation for the shielding effectiveness of enclosures with apertures", *IEEE Trans on Electromagnetic Compaticity*, Vol. 40, No. 3, 1998, pp. 240-247.